Failure mechanisms of concrete under impact loading

I. Vegt & K. van Breugel
Delft University of Technology, Delft, The Netherlands

J. Weerheijm
TNO Defence, Security and Safety, Rijswijk, The Netherlands
Delft University of Technology, Delft, The Netherlands

ABSTRACT: Numerical modelling can be used to predict the response of concrete structures under impact loading. To properly predict this response the rate dependency of concrete should be included in the numerical material model. The dimensional scale at which the fracture and energy absorption takes place influences the level of detail at which the concrete should be modelled. Therefore, the failure mechanisms under impact loading and the dependency of the failure mechanisms on the loading rate should be known. A combined computational and experimental research programme is performed at the Delft University of Technology. To fully understand the failure mechanisms, the data on mechanical properties are combined with stress-displacement curves and microscopic research of the fracture patterns. The results of the microscopic research and the reconstructed failure mechanisms are addressed in this paper.

1 INTRODUCTION

The response of concrete structures exposed to explosive and impulsive loading is an important safety issue. Numerical modelling can be used to predict the response of concrete structures under impact loading. However, concrete is a rate-dependent material (Körmeling et al. 1980, Weerheijm 1992). Therefore, a proper response prediction is only possible when the material behaviour of concrete and the failure mechanisms at high loading rates are known and understood.

At the Delft University of Technology (DUT) a combined computational and experimental research project is performed, dedicated to the response of concrete under high impact loading. The aim of this project is a physically realistic material model for concrete at high loading rates, which includes the rate dependency of concrete.

The material length scale, which is an important parameter in numerical modelling, is related to the material response and failure mechanisms. The key issue in the dynamic material response is the energy dissipation process by fracture at micro- and meso-level and the influence of the loading rate on the fracture process. The level at which the fracture and therefore the energy absorption takes place influences the scale at which the concrete has to be modelled. Therefore, the DUT- research aims to quantify the rate effect on the mechanical properties (strength and stiffness), as well as the load-displacement relation which reflects the fracture process and quantifies the fracture energy. This data is combined with microscopic research of the fracture patterns to learn about the rate effects on the fracture characteristics and the fracture mechanisms.

2 RATE DEPENDENCY OF CONCRETE

The rate dependency of concrete can be subdivided into two regimes; the regime with moderate rate effects for loading rates in the range from 10^{-4} GPa/s (static) up to 50 GPa/s, and the regime with extensive rate effects for loading rates beyond 50 GPa/s.

Micro-inertia effects in the fracture process zone mainly cause the rate dependency of concrete in the high regime (Weerheijm et al. 2003, 2004, Brara & Klepaczko 2006, in press). The moisture content is assumed not to be dominant in this regime. In the moderate regime, however, the moisture content is believed to play an important role in the strength increase of concrete (Rossi et al. 1992, Cadoni et al. 2001, Ross et al. 1996). From Vegt (2006b) it is concluded that not the moisture in the gel pores but the moisture in the capillary pores causes the rate effects in concrete. Although the influence of the moisture content in the moderate regime is recognized, it is not addressed in this paper.

The focus of the paper is the presentation of a full set of static and dynamic data for normally cured concrete and the analysis that leads to new knowledge on the dynamic failure mechanisms of concrete.

3 EXPERIMENTAL PROGRAM

3.1 *Experimental set-up*

To study the influence of the loading rate on the failure mechanisms and on the mechanical properties, experiments are conducted at three different loading rates; static loading rate (10^{-4} GPa/s) as a reference, medium loading rate with a Split Hopkinson Bar set-up (≈ 50 GPa/s) and high loading rates with a Modified Split Hopkinson Bar (> 1000 GPa/s).

3.2 *Specimens and concrete used*

The concrete specimens used for the different dynamic experiments are cylindrical specimens with a diameter of 74mm. The length of the specimens for the static and Split Hopkinson Bar (SHB) tests is 100mm. The specimens for the high loading rate tests have a length of 300mm. The specimens are drilled out of concrete cubes (rib length 200mm), at an age of 28 days. For the first 14 days, the cubes are kept in a controlled environment of 95% Relative Humidity (RH) and 20ºC. At day 14, they are moved to an environment of 50% RH and 20ºC. The specimens stay in this controlled environment (after being drilled out of the cubes) until the day of testing.

The composition of the concrete that is used for the specimens is similar to the concrete used in earlier research (Weerheijm 1992, Körmeling et al. 1980) in order to be able to compare the results from the experiments with results obtained in the past. For the cement a Portland cement (CEM I 32.5R) is used. The composition and the aggregate grading of the concrete are shown in Table 1 and Table 2.

Table 1. Composition of concrete.

	Cement	Aggregate	Water cement ratio	Air
	kg/m^3	kg/m^3	-	%
Mix A	375	1810	0.5	2.5

Table 2. Aggregate grading of concrete.

	8-16 mm	4-8 mm	2-4 mm	1-2 mm	0.5-1 mm	250-500 µm	125-250 µm
	%	%	%	%	%	%	%
Mix A	3	28	18	15	15	16	5

The mechanical properties of the concrete are determined at 28 days and 42 days (with the exception of the Young's modulus, which is only determined at 42 days). The compressive cubic strength and tensile splitting strength are determined with a standard cube (rib length 150mm), following the recommendations EN12390-3, EN-12390-4 and EN-12390-6. The average mechanical properties for the three different loading rates are summarized in Table 3. For the general characterization, all of the specimens were cured in a controlled environment until the day of testing: 95% RH and 20ºC.

Table 3. Average mechanical properties of concrete.

	Cube strength	Tensile split. strength	Young's modulus
	MPa	MPa	GPa
28 days	48.2	3.4	-
42 days	51.5	3.6	35.1

3.3 *The Split Hopkinson Bar*

The Split Hopkinson Bar (SHB) technique has been used to generate the moderate loading rates. The SHB set-up at the Delft University of Technology consists of two vertical cylindrical aluminium bars (diameter 74mm) with a total length of about 10m, between which the concrete specimen is glued (Figs. 1 and 2). The tensile stress wave is generated with a drop weight, which slides along the lower bar and hits an anvil at the end.

Figures 1 and 2. The Split Hopkinson Bar at the Delft University of Technology and a detail of the glued specimen and measurement system.

In the SHB set-up the strains are measured at the upper bar, while the total and elastic deformations are measured directly on the notched specimens with LVDT's (Linear Variable Differential Transducers) and strain gauges respectively. The signals are synchronised and combined to reconstruct the desired stress-displacement curve. The strength and fracture energy are quantified by this curve.

3.4 *The Modified Split Hopkinson Bar*

For the high loading rate regime (>1000 GPa/s), a new Modified Split Hopkinson Bar (MSHB) set-up is developed at TNO Defence, Security and Safety in

Rijswijk. The feasibility of the set-up was demonstrated by the TNO prototype test set-up (Weerheijm et al. 2003, 2004). The MSHB is based on a different principle than the SHB; the principle of spalling.

The MSHB set-up consists of a horizontal steel bar (length 2m, diameter 74mm), supported by strings (Fig. 3). The strings make sure that the rod can move freely and that the supports do not influence the wave propagation. The shock wave is introduced into the rod by detonating an explosive charge at one end of the bar. At the other end, a concrete specimen (length 300mm, diameter 74mm) is attached to the bar. The concrete specimen is first loaded in compression, but will fail in tension due to the reflected tensile wave (spalling).

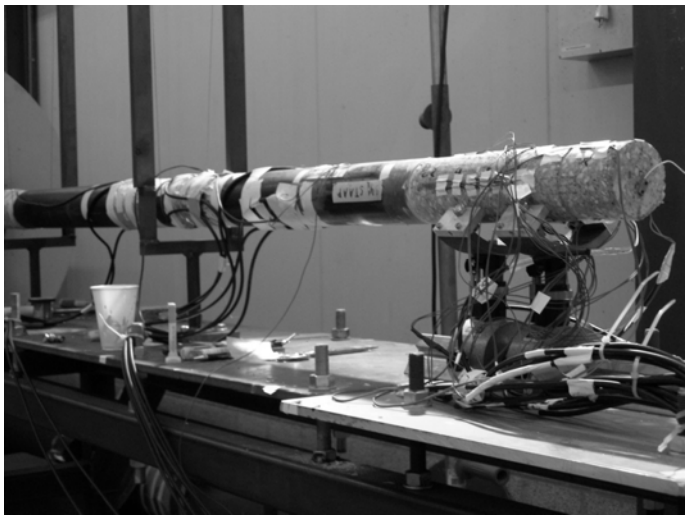

Figure 3. The Modified Split Hopkinson Bar set-up at TNO Defence, Security and Safety.

The measurement set-up of the MSHB is comparable to the set-up of the SHB. The transmitted pressure wave in the concrete specimen, the wave propagation and the reflection process are recorded with a number of strain gauges distributed along the notched specimen (Fig. 4). The applied load can be derived from the strain measurements on the incident bar and the specimen. The resulting stress at the failure zone (notch) is determined using the uniaxial wave theory to quantify the wave interaction process (Vegt 2006a, Vegt et al. 2007).

To be able to determine the stress-displacement curve, it is necessary to determine the deformation of the fracture zone directly. New deformation measuring devices have been developed, which can measure deformations at very high loading rates (Vegt 2006a, Vegt et al. 2007). The new device consists of a strain gauge glued onto a supporting synthetic foil (Fig. 5).

The measured deformations at the notch are combined with the resulting stresses in the notch to obtain the desired stress-displacement curve. The area under this curve represents the fracture energy.

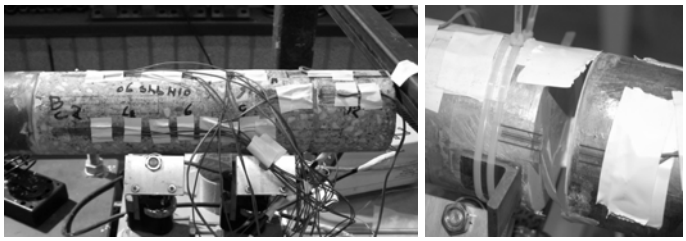

Figures 4 and 5. The concrete specimen of the MSHB with strain gauges and a detail of the new deformation measuring device with strain gauges on a supporting foil.

4 STRENGTH AND FRACTURE ENERGY

4.1 *Experimental data*

A set of static-, SHB- and MSHB tests has been performed and the derived data on strength and fracture energy are summarized in Table 4. Notice that the standard deviation of the fracture energy is very high for the MSHB tests.

The ratio between the dynamic tensile strength and the static strength reflects the rate dependency of concrete. This ratio for strength and fracture energy is presented in Table 5.

Table 4. Strength, fracture energy, number of succeeded tests and standard deviation (S).

	f_t	S	G_f	S	Tests
	MPa	MPa	N/m	N/m	-
Static	3.30	0.35	120	13.3	6
SHB	5.58	0.23	120	9.4	6
MSHB	17.0	1.31	1505	375	5

Table 5. Strength, fracture energy and loading rate and dynamic/static ratios.

	f_t	$/f_{t,Static}$	G_f	$/G_{f,Static}$	Loading rate
	MPa	-	N/m	-	GPa/s
Static	3.30	1.0	120	1.0	$1 * 10^{-4}$
SHB	5.58	1.7	120	1.0	39
MSHB	17.0	5.2	1505	12.5	1685

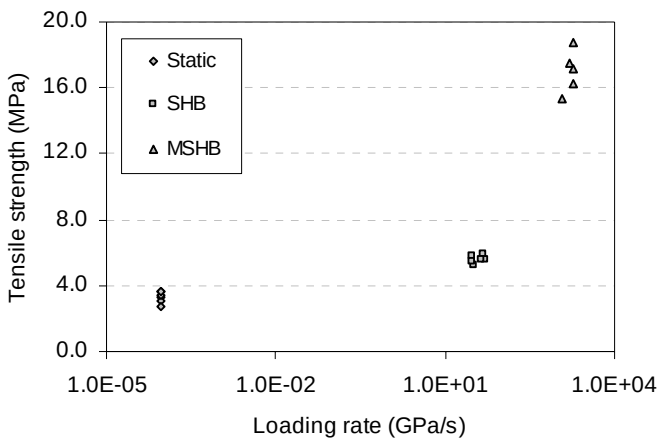

Figure 6. Tensile strength of static, SHB and MSHB tests plotted against the loading rate.

The tensile strength data is also presented in Figure 6. It is obvious that after reaching the loading rate threshold of about 50 GPa/s, the strength increase becomes more pronounced. The fracture energy does not increase when the loading rate increases in the moderate rate regime. However, in the high rate regime the fracture energy increases dramatically; the ratio between the high dynamic and static fracture energy is 12.5.

The data on average strength and dynamic/static strength ratio's in the moderate regime are comparable with literature (Cadoni et al. 2001, Rossi et al. 1992, Ross et al. 1996). Schuler (in press) finds a similar strength in the high loading rate regime. The ratio between the static and SHB fracture energy of 1.0 is also found by Weerheijm (1992). The very high increase in fracture energy in the high loading rate regime is similar to the results published by Brara & Klepazcko (in press). Schuler (in press) reports fracture energy data at high loading rates that are approximately three times lower.

4.2 *Stress-displacement curves*

Experimental data on the influence of the loading rate on the mechanical properties is the first step in studying the rate dependency of concrete. They reflect the dynamic response and failure process, but do not give sufficient insight in the fracture mechanisms or the dynamic behaviour. Therefore, not only the mechanical properties are determined from the experiments, but also the stress-displacement curves. The shape of the stress-displacement curves gives an indication of the failure behaviour. Examples of representative stress-displacement curves for the static, SHB and MSHB tests are shown in Figure 7.

Figure 7 shows that the modulus of elasticity increases when the loading rate increases, showed by the steeper ascending branch of the SHB and MSHB curves. Although the absolute fracture energy does not increase in the moderate loading rate regime, the stress-displacement curves of the static and SHB tests indicate a difference in failure mechanism. The first part of the descending branch of the SHB curve is steeper than the static curve. This indicates more brittle failure behaviour. The tail of the curve seems not to be affected by the higher loading rate.

The MSHB curve obviously has a larger area under the stress-displacement curve and therefore the fracture energy is high (Fig. 7). The peak of the MSHB curve is very wide and the pre-peak nonlinearity of the MSHB curve is higher than for the other two curves. These features might be caused by an initial process of extensive micro cracking that finally results in the formation of single or multiple macro-cracks. The presence of many propagating micro-cracks causes a growth in damage of the material, and therefore in the energy absorption, until the formation of macro-cracks takes place.

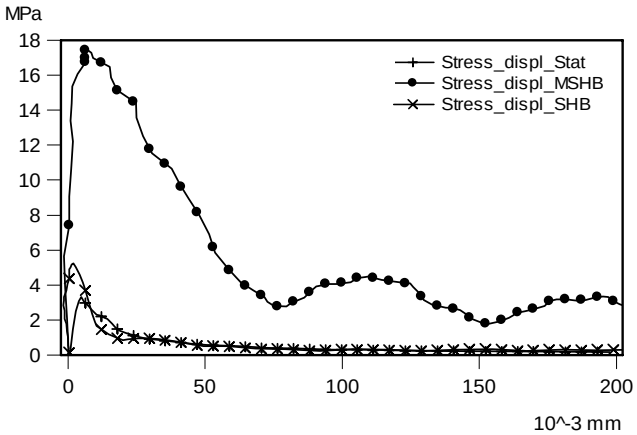

Figure 7. Examples of representative stress-displacement curves for static, SHB and MSHB tests.

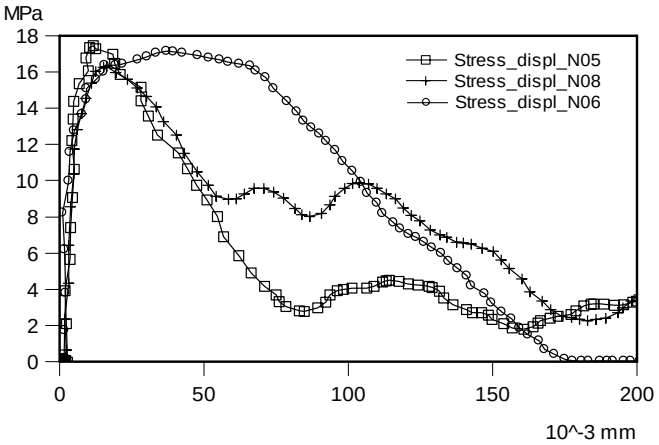

Figure 8. Stress-displacement curves for three MSHB tests.

In comparison with the other test conditions, the shape of the stress-displacement curves of the individual MSHB varies considerably (Fig. 8). It seems that the fracture behaviour of the concrete specimens at very high loading rates differs per test. A very wide peak, like in test MSHB-N06 (Fig. 8) indicates that more than one macro crack is formed, before the specimen is completely broken at the notch.

The stress-displacement curve represents the material and the structural response. At the high loading rates the influence of the inertia effects related to the structural response might become more pronounced than for the other loading rates. The effect exhibits most when the macro cracks are formed and the separation process occurs.

The "bumps" in the curves of the MSHB tests (Fig. 8) illustrate the presence of structural behaviour in the stress-displacement curves. It indicates that the macro-crack is not formed fast enough to prevent a returning wave from interfering with the strain measurements just past the notch, which are used to determine the stress-displacement curve. When a crack starts to grow in the notch, part of the tensile wave is reflected as a compressive wave and moves back to the end of the specimen. At this free end, the wave is again reflected as a tensile wave

and starts moving towards the notch again. When the notch is not completely broken at the time this returning wave pulse arrives, this "new" returning wave can pass the notch and interfere with the strain measurements past the notch. The time to travel upen down the end of the specimen is about 35 to 40 μs. This is also approximately the time between the highest peak and the peak of the first bump in the strain measurements just pasted the notch.

Apparently the stress-displacement curve is affected by structural response, resulting in too high fracture energy values.

5 FAILURE MECHANISMS

5.1 *Failure at macro-scale*

Although the stress-displacement curves give an indication of the failure mechanisms, to fully understand the rate dependency of the dynamic failure behaviour of concrete it is necessary to study the crack patterns in detail. Therefore, after the dynamic experiments are finished, the specimens are impregnated with a fluorescent epoxy. After impregnation, the specimens were sawn in half to be able to study the macro-crack patterns.

From Figures 9 and 10 can be concluded that the macro-crack patterns of the static and the SHB tests are not that different, although the static cracks seem to be a little more whimsical. In both cases, almost no fractured aggregates were detected and most of the aggregate particles were pulled out of the cement paste. The particles that were fractured had a low density and probably had a lower strength than the cement paste. The few fractured particles were observed both in the static tests and the SHB tests.

The macro-crack patterns of the MSHB tests differ per test. Sometimes the width of the zone with macro-cracks seems to be very small and other times the width is larger and the cracks are more whimsical (Figs. 11 and 12). The characteristics of the macro-crack correspond with the shape of the stress-displacement curves; when the peaks of the curves are wider, which indicates multiple fractures, the width of the zone with macro-cracks seems to increase (Figs. 8, 11 and 12).

A comparison between the macro-crack patterns of the static and SHB tests and the crack patterns of the MSHB tests is difficult, since the characteristics of the macro-crack in the MSHB tests are not always the same. One major difference can be observed; the amount of fractured aggregate particles. In the MSHB tests more aggregates are fractured, than in the other two loading conditions. However, the cracks not always run through the aggregate particles but also move around them, searching for the weakest part of the cement paste close to the particles; the interfacial transition zone (ITZ).

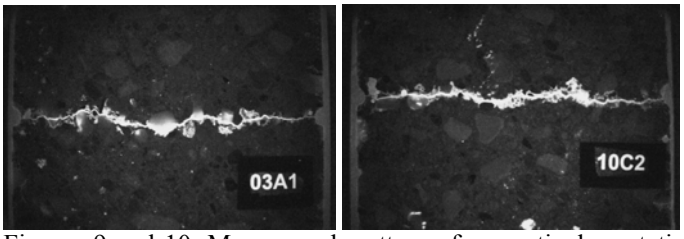

Figures 9 and 10. Macro-crack pattern of respectively a static test and a SHB test.

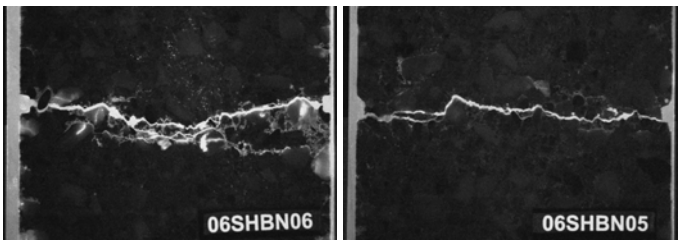

Figures 11 and 12. Macro-crack patterns of two different MSHB tests.

From the macro-crack patterns it can be concluded that there is no difference in fracture behaviour between the static and SHB tests, although the shape of the stress-displacement curves indicates there should be small differences. The observations at macro-level show that more than one fracture mechanism can take place in the high loading rate regime. By studying the cracks on macro-level only, the differences between the stress-displacement curves cannot be explained and the fracture mechanisms cannot be determined. Therefore, the cracks were studied in more detail with so called thin-sections.

5.2 *Failure at micro-scale*

Thin-sections are very thin slices of concrete (≈60μm), which allow us to study not only the detailed characteristics of the macro-cracks but also the existence of micro-cracks around the macro-crack. The size of the thin-sections is about 30mm to 45mm. To cover the complete crack in a specimen, two thin-sections are situated next to each other.

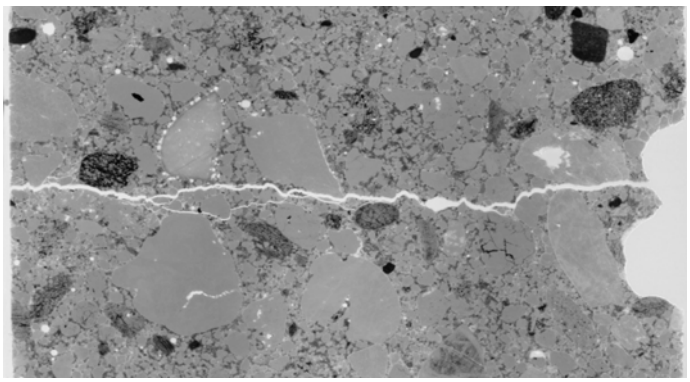
Figure 13. Thin-section of the fracture zone of a static test (3D2-Right).

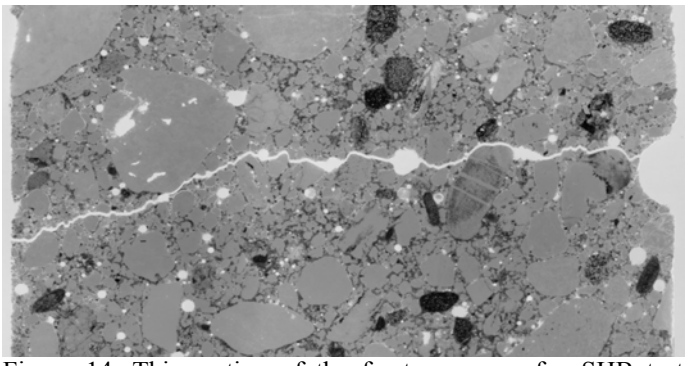

Figure 14. Thin-section of the fracture zone of a SHB test (10A2-Right).

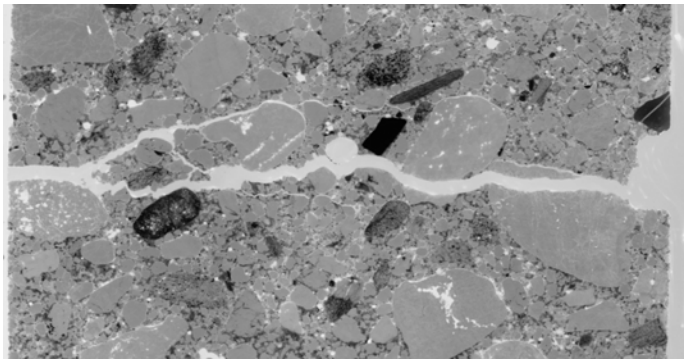

Figure 15. Thin-section of the fracture zone of a MSHB test (N07-Right).

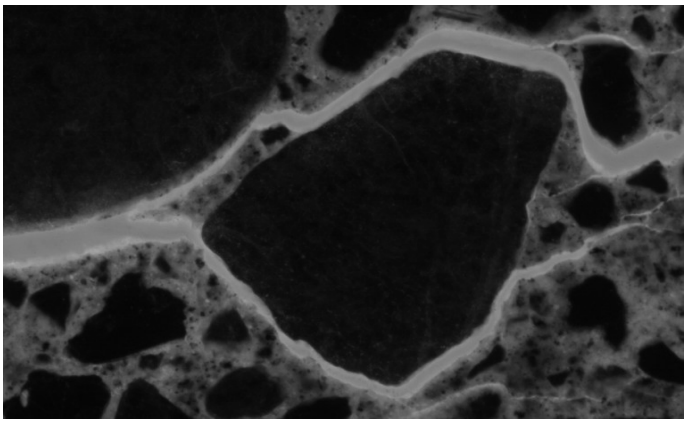

Figure 16. Bridging of crack-tips in static tests (3D2-Left), magnification 10x.

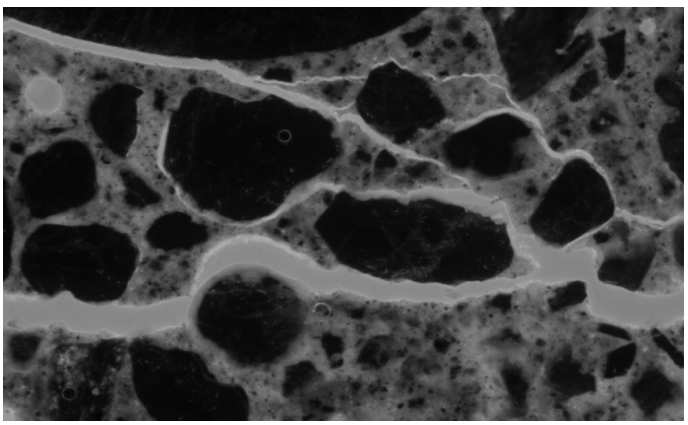

Figure 17. Macro- and micro-cracks in static tests (3D2-Right), magnification 5x.

First, the crack patterns of the thin-sections are studied using black-light, shining through the thin-sections (Figs. 13, 14 and 15). The white colour in the thin-sections corresponds with voids or cracks that are filled with epoxy. When comparing the thin-sections of the static and SHB tests, it is clear that the static tests have a higher amount of smaller cracks linked to the macro-crack. The thin-sections of the MSHB tests show not only a higher amount of small cracks, but also a lot of micro-cracks. These micro-cracks are discovered along the total area of the thin-section and indicate that the fracture zone of the high loading rate regime is at least 30mm.

Micro- and macro-cracks can be made even more visible by zooming in with an optical microscope. The optical microscope used to study the thin-sections at higher magnifications, has different options for types of light and filters. A black light is used in combination with a certain orange filter, to highlight the cracks while the aggregate particles are dark (Fig. 16). The cement paste has a higher porosity than the aggregate particles and therefore has a colour in between of the dark colour of the particles and bright colour of the cracks.

The thin-sections of the static tests show that in static tests the cracks are branching and bridging. This means that cracks grow from different directions and are trying to find each other to form a large macro-crack. Because the cracks in the static tests are naturally searching for the weakest spot, they are mostly propagating around the aggregate particles and following the ITZ, the interface between the cement paste and the aggregate particles. Therefore, two cracks can run around an aggregate particle before one of the crack tips reaches the other crack, so called bridging (Fig. 16). The static thin-sections show a large amount of small cracks close to the final macro-crack (Fig. 17), which is in accordance with the crack-branching principle (van Mier 1997). Occasionally, a isolated micro-crack is detected on a short distance from the macro-crack.

From the thin-sections of the SHB tests can be concluded that the crack patterns are similar to the static crack patterns. Small cracks can be found around the macro-crack. However, the amount of small cracks is lower than for the static tests and the width of the fracture zone is much smaller. No evidence can be found that crack bridging between larger cracks has occurred, only initial branching of small cracks is observed (Fig. 18). The connected and isolated micro-cracks are situated at a short distance from the macro-crack (Fig. 18). Occasionally an aggregate particle is fractured, when the strength of the particle is low (Fig. 19).

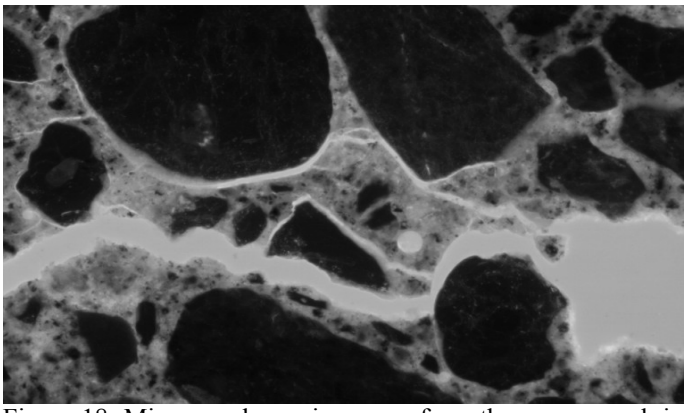

Figure 18. Micro-crack moving away from the macro-crack in SHB test (10A4-Left), magnification 5x.

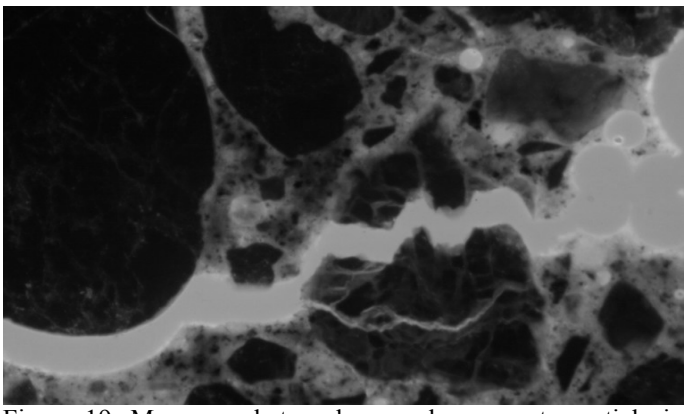

Figure 19. Macro-crack trough a weak aggregate particle in SHB test (10A2-Left), magnification 10x.

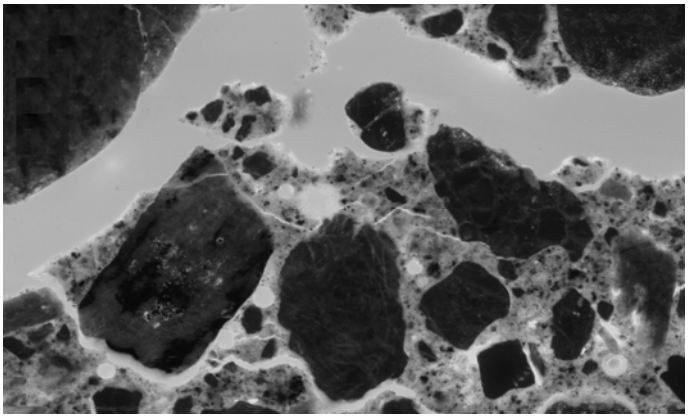

Figure 20. Macro-crack surrounded by smaller cracks and micro-cracks, in MSHB test (N07-Left), magnification 5x.

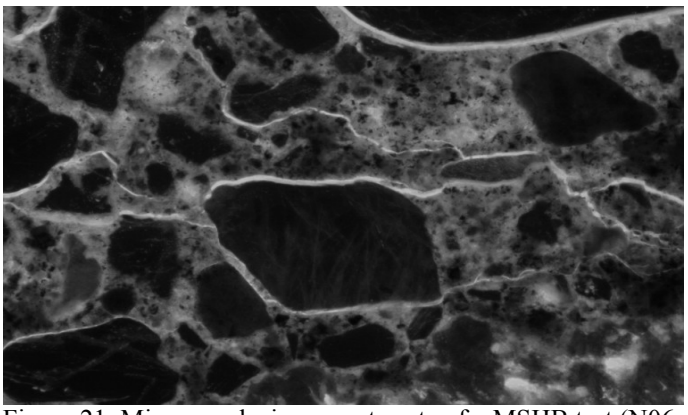

Figure 21. Micro-cracks in cement paste of a MSHB test (N06-Left), Magnification 10x.

The thin-sections of the MSHB tests show a lot of isolated micro-cracks, not only surrounding the aggregate particles but also through the cement paste (Fig. 21). These isolated micro-cracks are not connected to the macro-crack and can be found close to the macro-crack as well as further away, up to the edges of the thin-sections.

The micro-cracks develop into macro-cracks which propagate trough the material, even through the aggregate particles. More broken aggregate particles are found than in the static and SHB tests. Not only macro-cracks run through the particles, micro-cracks also split aggregate particles into pieces (Fig. 20). The particles that are broken are not necessarily weak particles; cracked particles with high densities (very dark colour) are also discovered.

The difference between the individual MSHB tests is found in the number of macro-cracks. In all the MSHB tests, smaller cracks connected to the macro-crack are observed. However, some test show a lot of these connected cracks (N06), and some only a few (N05).

5.3 *Failure mechanisms*

From the microscopic analysis of the fracture zone, the failure mechanisms at different loading rates can be reconstructed and the influence of the loading rate on the failure behaviour of concrete determined.

Under static loading conditions crack branching and bridging takes place. The experimental set-up is partly to blame for this behaviour. The static test set-up has non-rotational loading platens. This means that the platens stay parallel during testing. The crack starts to develop from the weakest spot along the circumference of the specimen. Because the loading platens are forced to remain parallel during the experiment, a closing bending moment develops. The bending moments prevent the crack from further extension, until the other side of the specimen starts to fracture. The two crack tips tend to avoid each other, until they finely meat. This is called branching and bridging of cracks, for which evidence is observed in the thin-sections. Due to the low loading rate, the cracks have a lot of time to develop, searching for the weakest spots, and therefore are running around the aggregate particles. The crack branching and redistribution of stresses that takes places during the failure process makes this failure behaviour more ductile than the SHB failure, which is also shown in the stress-displacement curves.

Although the fracture energy of the SHB tests is the same as the static tests, the fracture behaviour is somewhat different. The SHB-test is not deformation controlled and time for stress redistribution is limited, therefore crack bridging will not occur. The thin-sections indicate that the crack starts at a certain point along the circumference of the specimen, propagating trough the specimen until the specimen

is fully broken. The initial crack can split in more than one crack while propagating, but only one crack grows into a macro-crack, the other cracks are small cracks connected to the macro-crack. The amount of connected cracks and the width of the fracture zone are smaller than for the static tests, indicating a more brittle behaviour in comparison to the static loading rate.

In the MSHB tests, the loading rate is very high and the cracks have less time to search for the weakest spots in the cement paste, the ITZ. Therefore, the cracks do not only run around the aggregate particles, but also run through them. The fracture of aggregate particles increases the amount of energy demanded for the failure of the specimen. However, it does not cover the large increase of fracture energy measured in the MSHB tests. The high increase in fracture energy is caused by the many micro-cracks that develop under high impact loading. The presence of many propagating micro-cracks causes a growth of damage in the material and therefore also in the energy absorption, until macro-cracks develop. The amount of macro-cracks differs per test; sometimes multiple macro-cracks develop and other times only one single macro-crack is observed (Figs. 11 and 12). The fracture energy of the specimen is directly related to the amount of micro cracking, but probably also by the number of macro-cracks. For example, test N06 has a fracture energy of 1860 N/m, compared to 1190 N/m for test N05, which has only one visible macro-crack and a few surrounding smaller cracks. This fracture behaviour at high impact tensile loading is very different than the static and SHB behaviour, resulting in a higher tensile fracture energy.

6 CONCLUSIONS

The influence of the loading rate on concrete behaviour is studied in a combined experimental and computational research programme. To understand the dynamic response and identify the dominant failure mechanisms it is necessary to quantify the rate effects on strength and fracture energy as well as the stress-displacement relation for a single fracture zone. This quantitative data has to be combined with microscopic research of the fracture patterns to determine the amount of micro cracking and the width of the failure zone. The first results of this approach are given in the paper for three loading rates; static, medium (SHB) and high loading rate (MSHB).

The static and SHB fracture mechanisms are similar. The main difference is the crack bridging process in the static tests, making the failure behaviour more ductile than in the SHB tests. The failure of the MSHB is dominated by the existence of many propagating micro-cracks, developing into one or more macro-cracks. The energy dissipation is very high in this high loading rate regime and is dominated by fracture at micro-scale in stead of macro-scale. For the MSHB-test condition, the stress-displacement relation derived from the raw experimental data is biased by inertia effects in the structural response, resulting in too high values for the fracture energy.

It is very important that the length-scale of the numerical model is proportional to the width of the zone of micro cracking. Furthermore, when the aim is to simulate the fracture process itself, the aggregate particles, ITZ and cement paste should be modelled separately to properly model the dominant failure mechanism of concrete under impact tensile loading.

REFERENCES

Brara, A. & Klepaczko, J.R. 2006. Experimental characterization of concrete in dynamic tension. *Mechanics of Materials* 38: 253-267.

Brara, A. & Klepaczko, J.R. In press. Fracture energy of concrete at high loading rates in tension. *Int. J. of Impact Engineering.*

Cadoni, E. & Labibes, K. & Albertini, C. & Berra, M. & Giangrasso, M. 2001. Strain rate effect on the tensile behaviour of concrete at different relative humidity levels. *Materials and Structures* 34: 21-26.

Körmeling, H.A. & Zielinsky, A.J. & Reinhardt, H.W. 1980. *Experiments on concrete under single and repeated uniaxial impact tensile loading*. Delft: Delft University of Technology.

Mier van, J. 1997. *Fracture processes of concrete.* CRC Press.

Ross, A.C. & Jerome, D.M. & Tedesco, J.W. & Hughes, M.L. 1996. Moisture and strain rate effects on concrete strength. *ACI Materials Journal* 93(3): 293-300.

Rossi, P. & van Mier, J.G.M., & Boulay, C. & le Maou, F. 1992. The dynamic behaviour of concrete: influence of free water. *Materials and Structures* 25: 509-514.

Schuler, H. & Mayrhofer, C. & Thoma, K. In press. Spall experiments for the measurement of the tensile strength and fracture energy of concrete at high strain rates. *Int. J. of Impact Engineering.*

Vegt, I & Weerheijm, J. 2006a. Dynamic response of concrete at high loading rates – A new Hopkinson Bar device. *Proceedings of the Int. Conf. Brittle Matrix Composites (BMC8), Warsaw, Poland, October 2006*.

Vegt, I. & Weerheijm, J. & Van Breugel, K. 2006b. Moisture content and the effect on dynamic concrete behaviour. *Proceedings of the 2nd Int. Conf. on Design and Analysis of Protective Structures, Singapore, 13-15 November 2006.*

Vegt, I. & Weerheijm, J. & Van Breugel, K. 2007. The fracture energy of concrete under impact tensile loading- a new experimental technique. *Subjected to CONSEC Conference June 2007, Tours, France.*

Weerheijm, J. 1992. *Concrete under impact tensile loading and lateral compression*. Thesis. Rijswijk: TNO.

Weerheijm, J. & van Doormaal, J.C.A.M. & van de Kasteele, R.M. 2003. *Development of a new test set-up for dynamic tensile tests on concrete under high loading rates. Part 2: Results and evaluation of test series B and C on concrete*. Rijswijk:TNO.

Weerheijm, J. & van Doormaal J.C.A.M. 2004. Tensile failure at high loading rates; Instrumented spalling tests. *International Conference FramCoS 5, April 2004*.